

Production of $D^{*+}(2010)$ mesons by high energy neutrinos from the Tevatron

E632 Collaboration^{1–20}

A.E.Asratyan¹¹, M.Aderholz¹³, V.V.Ammosov⁸, M.Barth³, H.H.Bingham^{1*}, E.B.Brucker¹⁹,
 R.A.Burnstein⁹, T.K.Chatterjee⁵, E.C.Clayton¹⁰, P.F.Ermolov¹⁴, I.N.Erofeeva¹⁴, P.J.W.Faulkner²,
 G.S.Gapienko⁸, J.Guy¹⁷, J.Hanlon⁶, G.Harigel⁴, A.A.Ivanilov⁸, V.Jain^{7†}, G.T.Jones², M.D.Jones⁷,
 T.Kafka²⁰, V.S.Kaftanov¹¹, M.Kalekar¹⁶, J.M.Kohli⁵, V.M.Korablev⁸, M.A.Kubantsev¹¹,
 M.Lauko¹⁶, J.Lys¹, S.I.Lyutov¹⁴, P.Marage³, R.H.Milburn²⁰, I.S.Mittra⁵, D.R.O.Morrison⁴,
 V.I.Moskalev¹¹, V.S.Murzin¹⁴, G.Myatt¹⁵, R.Naon⁹, D.Passmore²⁰, M.W.Peters⁷, H.Rubin⁹,
 J.Sacton³, J.Schneps²⁰, J.B.Singh⁵, S.Singh⁵, W.Smart⁶, P.Stamer^{16‡}, E.S.Vataga¹⁴,
 K.E.Varvell^{2#}, W.Venus¹⁷, S.Willocc^{20§}

Abstract

Charged vector $D^{*+}(2010)$ meson production is studied in a high energy neutrino bubble chamber experiment with mean neutrino energy of 141 GeV. The D^{*+} are produced in $(5.6 \pm 1.8)\%$ of the neutrino charged current interactions, indicating a steep increase of cross section with energy. The mean fractional hadronic energy of the D^{*+} meson is 0.55 ± 0.06 .

- [1] University of California, Berkeley, California 94720, USA.
- [2] University of Birmingham, Birmingham B15 2TT, UK.
- [3] Inter-University Institute for High Energies, ULB–VUB, B–1050 Brussels, Belgium.
- [4] CERN, CH–1211 Geneva 23, Switzerland.
- [5] Panjab University, Chandigarh 160014, India.
- [6] Fermilab, P.O.Box 500, Batavia, Illinois 60510, USA.
- [7] University of Hawaii, Honolulu, Hawaii 96822, USA.
- [8] Institute of High Energy Physics, RU-142284, Protvino, Moscow Region, Russia.
- [9] Illinois Institute of Technology, Chicago, Illinois 60616, USA.
- [10] Imperial College of Science and Technology, London, SW7 2AZ, UK.
- [11] Institute of Theoretical and Experimental Physics, RU-117259 Moscow, Russia.
- [12] University of Jammu, Jammu 180001, India.
- [13] Max-Planck-Institut für Physik, 80805 München, Germany.
- [14] Moscow State University, RU-119899 Moscow, Russia.
- [15] Department of Nuclear Physics, Oxford, OX1 3RH, UK.
- [16] Rutgers University, New Brunswick, NJ 08903, USA.
- [17] Rutherford Appleton Laboratory, Chilton, Didcot, OX11 0QX, UK.
- [18] DPhPE, Centre d'Etudes Nucléaires, Saclay, F–91191 Gif sur Yvette, France.
- [19] Stevens Institute of Technology, Hoboken, New Jersey 07030, USA.
- [20] Tufts University, Medford, Massachusetts 02155, USA.

* Deceased.

† Present address: Wilson Lab., Cornell University, Ithaca, NY 14853.

‡ Permanent address: Seton Hall University, S. Orange, NJ 07079, USA.

Present address: Now at ANSTO, Menai NSW 2234, Australia.

§ Present address: SLAC Bin 96, P.O. Box 4349, Stanford, CA 94309.

To be submitted to Zeitschrift für Physik C

1 Introduction

This paper reports a study of $D^{*+}(2010)$ production by high energy neutrinos using bubble chamber techniques. Dimuon studies using electronic techniques do not distinguish between various charm fragmentation channels (D , D^* , D_s , D_s^* , Λ_c , *etc.*), and rely on model predictions in deriving the cross section of charm production by neutrinos. More detailed information is provided by tracking devices such as bubble chambers permitting mass reconstruction of various charmed particles, either with or without secondary vertex recognition.

The Fermilab 15 foot Bubble Chamber with a neon–hydrogen filling was irradiated by a neutrino beam with quadrupole–triplet focusing from the Tevatron which was aimed at obtaining the highest neutrino energies [1]. The neutrino– and antineutrino– induced charged-current interactions are in a ratio of 6 to 1, and have mean energies of 141 and 110 GeV. Only the neutrino component of the beam (producing D^{*+} rather than D^{*-} mesons) is considered here. In the 1985 and 1987 data taking runs for this experiment, E632, the molar neon concentration was 74.0 and 62.5 per cent, respectively. Muons with momentum over 5 GeV from interactions in the bubble chamber are selected after crossing an absorber by hits in the counter planes of the External Muon Identifier. These muons are identified with an efficiency of 91%, while the background from hadron punchthrough, meson decays, and accidental association does not exceed 0.7%. There are 5243 neutrino–induced charged current interactions selected from the ‘minimum bias’ event sample formed by measuring all neutrino interactions on part of the film. More of the film was scanned for events with visible decays of neutral strange particles, which were then fully measured (the ‘ V^0 ’ sample). This additional sample effectively increases the statistics of events with observed K_S^0 decays by a factor of 1.63.

The bubble chamber was equipped with a holographic camera, but this information is not used in this study as it is only available for events in a limited volume. As secondary vertices from weak decays of charmed particles are normally not resolved on conventional film, one has to rely on combinatorial mass selection of their decay products, usually involving strange particles. Note that while the neutral kaons are identified in the bubble chamber by the $K_S^0 \rightarrow \pi^+\pi^-$ decays [1], the charged kaons are essentially indistinguishable from pions. Therefore, all charged particles are treated as possible pions and as possible kaons, unless identified otherwise (as low momentum protons stopping in the bubble chamber or electrons losing energy by photon bremsstrahlung). Only charged particles and K_S^0 mesons with measured fractional momentum uncertainty, σ_p/p , below 20%, and gammas with σ_p/p below 40%, are used for mass reconstruction to ensure acceptable precision; a correction for events failing these selections is detailed in section 4.

2 Selection of D^0 decay and $D^{*+} \rightarrow \pi^+ D^0$ candidates

We select the candidates (called X^0) for weak decays of the $D^0(1864)$ in the decay channels

$$D^0 \rightarrow K^-\pi^+ \tag{1}$$

$$\rightarrow K_S^0\pi^+\pi^- \tag{2}$$

$$\rightarrow K^-\pi^+\pi^0 \tag{3}$$

$$\rightarrow K^- \pi^+ \pi^- \pi^+ \quad (4)$$

$$\rightarrow K_s^0 \pi^+ \pi^- \pi^0 \quad (5)$$

All possible pairs of gammas with mass within three standard deviations of 135 MeV are taken as candidates for the π^0 in (3) and (5). In all channels, the mass of a pion system recoiling against a kaon is required to be less than 1.4 GeV, the kinematic boundary for D^0 decays.

In order to reduce combinatorial backgrounds to the D^0 signal, further selections are made on the decay products. Candidates for decays (1), (3), and (4) are dropped when the K^- meson candidate travels in the very forward or very backward directions in the X^0 rest frame with respect to the X^0 boost direction from the lab (*i.e.*, $|\cos\theta| > 0.9$).

The decay $D^0 \rightarrow K^- \pi^+ \pi^0$ is known to be dominated by the intermediate resonant states $K^- \rho^+$, $\bar{K}^{*0} \pi^0$, and $K^{*-} \pi^+$ [2]. Accordingly, in selecting (3) we demand that either $m(\pi^+ \pi^0)$ be within ± 150 MeV of the central ρ^+ mass value, or one of the $K\pi$ masses be within ± 80 MeV of the corresponding K^* central mass value. Additionally, the decay helicity angle β is constrained by $|\cos\beta| > 0.7$. (In a two-stage decay $D^0 \rightarrow VP$, $V \rightarrow P_1 P_2$, β is defined as the angle between P and P_1 directions in the intermediate V rest frame. In the P-wave decays discussed, the $\cos\beta$ distribution is proportional to $\cos^2\beta$.) The acceptance of this helicity angle cut is 0.66.

The decay $D^0 \rightarrow K^- \pi^+ \pi^- \pi^+$ is dominated by resonant states yielding a ρ^0 [2]: $K^{*0} \rho^0$ and $K^- a_1^+$ where $a_1^+ \rightarrow \rho^0 \pi^+$. As a result, the mass of the higher-mass $\pi^+ \pi^-$ pair peaks near 770 MeV [3]. Accordingly, in (4) we require the higher-mass $\pi^+ \pi^-$ pair to be in the mass range between 650 and 900 MeV. From reference [3], we expect that the acceptance of this cut is 0.65.

We select the $D^{*+} \rightarrow \pi^+ D^0$ candidates, by requiring the measured mass difference, $r = m(\pi^+ X^0) - m(X^0) - m(\pi^+)$, to be within three standard deviations of 5.85 MeV [2].

Both the experimental error on r and the phase space show a steep increase towards higher r values, resulting in a high level of background combinations arising from the high- r region. To constrain the latter, for r values in excess of 5.85 MeV, the error on r is computed after rescaling the slow pion 3-momentum to fit the correct value of mass difference. (The rescale effectively determines the π^+ momentum in the D^0 frame, but not its angles there. However, we have verified that the ‘rescaled’ error on r is insensitive to these angular degrees of freedom. For definiteness, we use a procedure not affecting the π^+ angle in the D^0 rest frame.) The validity of the rescale procedure is supported by a Monte Carlo simulation reproducing our experimental resolutions. *A posteriori*, it is also justified by non-observation of a significant leakage of the signal into mass difference sidebands, see below.

In the $D^0(1864)$ mass region, the uncertainty on the mass of the decay products, $m(X^0)$, is ± 55 MeV on average, and exceeds 100 MeV for 10% of all events. The mean uncertainty on the mass difference r is ± 3.3 MeV.

3 The D^{*+} Signal and Production Dynamics

The masses of selected X^0 combinations tagged by a slow π^+ (*i.e.*, satisfying the $D^* - D$ mass difference condition) are plotted in Fig 1 for D^0 decay channels (1)-(4) as listed above; channel (5) has no candidates. One event gives two $X^0 = K^- \pi^+ \pi^- \pi^+$ contributions to the D^0 mass region within three standard deviations of $D^0(1864)$.

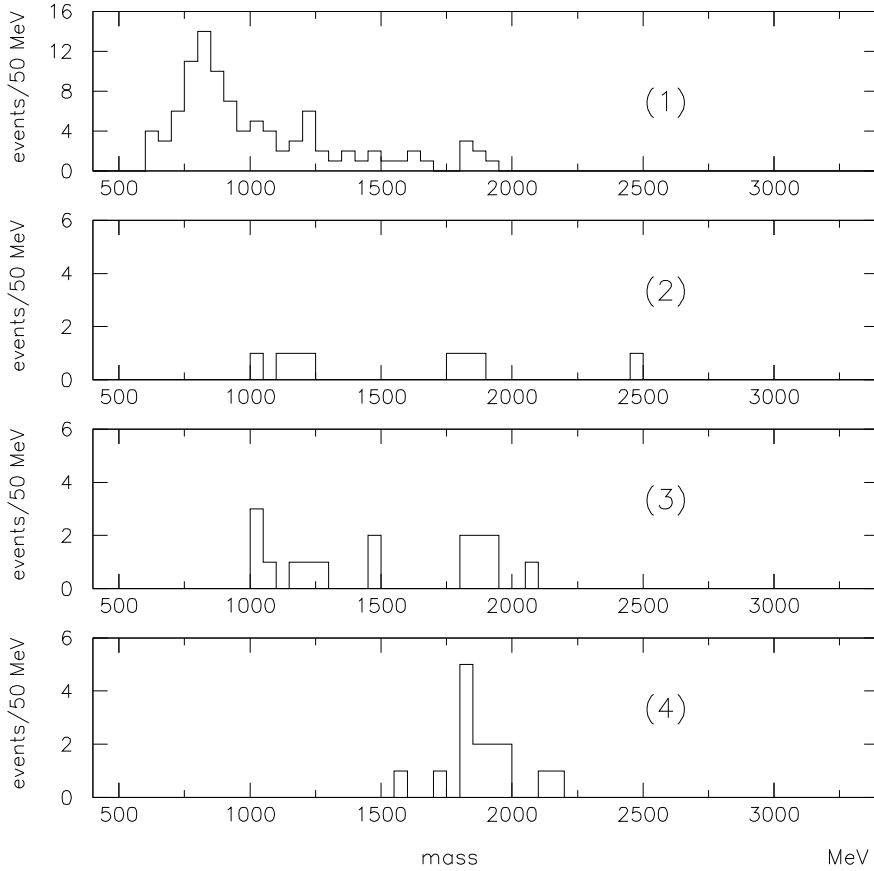


Figure 1: Masses of X^0 combinations passing the D^*-D mass difference selection for: (1) $X^0 = K^- \pi^+$; (2) $K_S^0 \pi^+ \pi^-$; (3) $K^- \pi^+ \pi^0$; (4) $K^- \pi^+ \pi^- \pi^+$; while (5) $K_S^0 \pi^+ \pi^- \pi^0$ has no candidates.

The combined mass distribution depicted in Fig 2a shows an enhancement in the $D^0(1864)$ mass region. No enhancements are observed in mass distributions with either a wrong-sign (negative) slow pion shown in Fig 2b, or with a right-sign pion in the D^*-D mass difference sidebands between 3 and 6 standard deviations, see Fig 2c.

Fig 3a shows the corresponding ‘detachment’ variable defined as $m(X^0) - m(D^0)$ divided by the error on $m(X^0)$, thus measuring the distance between the two masses in terms of standard deviations. Fig 3a verifies that the width of the peak is compatible with the experimental resolution. This distribution is then fitted to a sum of a linear background and a Gaussian with position and width fixed at expected values of zero and unity, respectively. (In a fit treating them as free parameters, we obtain $+0.11 \pm 0.25$ for peak position, and 0.89 ± 0.16 for its width.) The fitted signal is 18.7 ± 4.8 combinations above the background. Similar fits to the background plots Figs 3b and 3c yield signals of $+1.3 \pm 2.0$ and $+1.5 \pm 2.4$ which are compatible with zero.

For comparison with the background, we then select the 24 peak combinations within three standard deviations of $m(D^0)$, retaining only the combination closest to $m(D^0)$

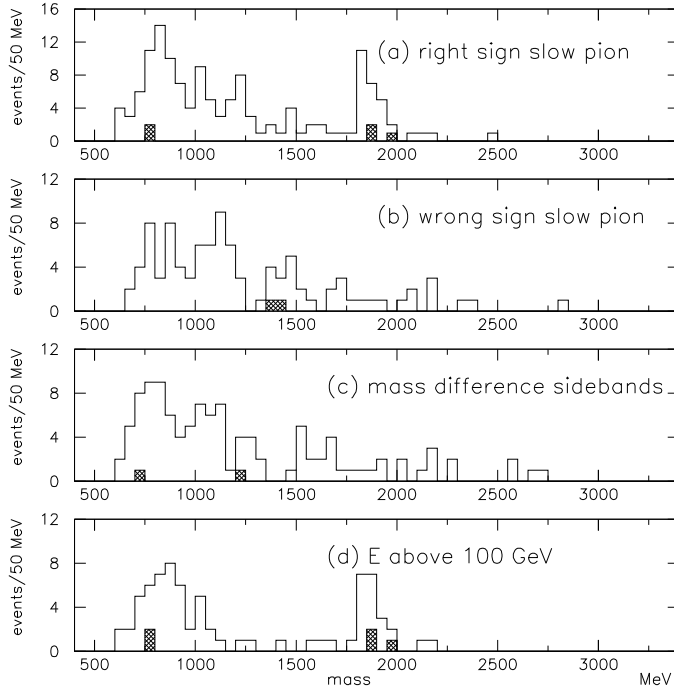


Figure 2: Combined $m(X^0)$ plots for : (a) X^0 combinations tagged by a right-sign slow pion passing the D^*-D mass difference selection; (b) X^0 combinations tagged by a wrong-sign slow pion passing the mass difference selection; (c) X^0 combinations tagged by a right-sign pion with mass difference in the sidebands; (d) same as (a) but for $E_\nu > 100$ GeV. The shaded entries are from the V^0 sample not involving a decay K_S^0 , but accompanied by an additional detected K_S^0 .

for the double entry mentioned above. We consider three background samples, selecting combinations within ± 400 MeV of $m(D^0)$ in Figs 2a, 2b, and 2c, and then excluding the peak combinations from Fig 2a. The mean value of visible fractional hadronic energy of the peak D^* candidates, $\langle z_{vis} \rangle = 0.58 \pm 0.04$, significantly exceeds that for the combined background, $\langle z_{vis} \rangle = 0.41 \pm 0.03$. (The individual values for the three backgrounds are all compatible within one standard deviation.)

To probe the dynamics of D^{*+} production, one must first correct the visible neutrino energy for undetected neutrals. (Note that for these events, none of the usual statistical corrections based on all charged current events can be applied, as the D^{*+} is expected to carry the bulk of hadronic energy.) We correct the neutrino energy using

$$E_\nu = P_L^\mu + R * P_L^h,$$

where P_L^μ and P_L^h are the longitudinal momenta of the muon and of the sum of all measured hadrons, and R is the average correction factor based on transverse momentum balance.

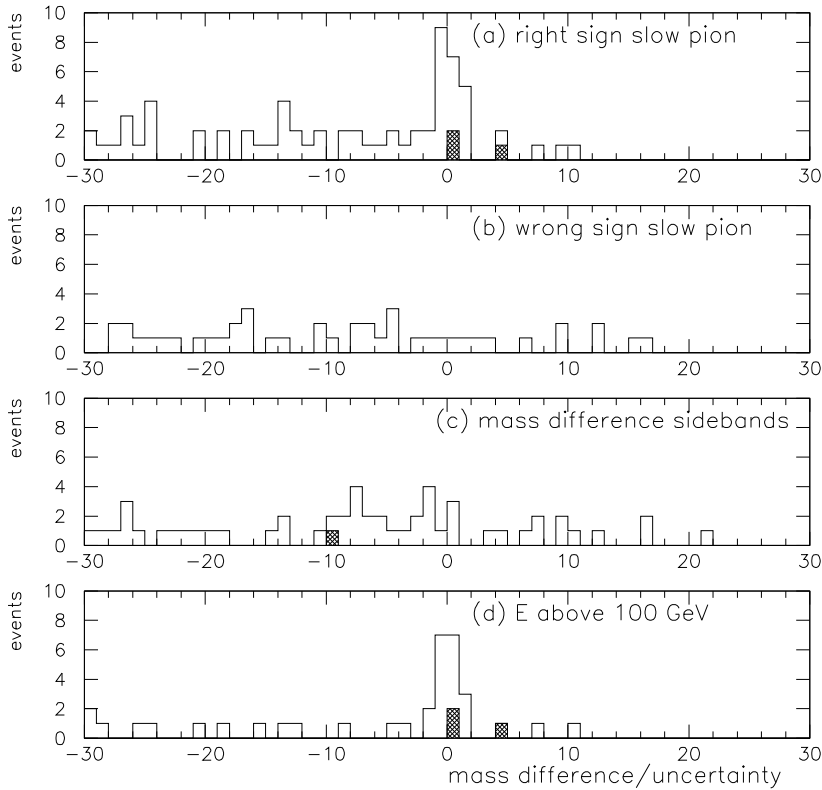


Figure 3: The ‘detachment’, $[m(X^0) - m(D^0)]/\sigma_m$ (see text) for the same combinations as in Fig 2.

We derive the value of R by analysing the asymmetry, a , between the muon transverse momentum with respect to incident neutrino, P_T^μ , and the sum of all measured hadrons transverse momenta in the neutrino-muon plane, P_T^h :

$$a = (P_T^\mu - P_T^h)/(P_T^\mu + P_T^h).$$

For the 24 selected peak combinations, we obtain a mean value $\langle a \rangle = 0.069 \pm 0.040$, which gives the correction factor

$$R = (1 + \langle a \rangle)/(1 - \langle a \rangle) = 1.15 \pm 0.09.$$

After neutrino energy correction, we obtain the ‘true’ fractional hadronic energy, z , for the peak and background D^{*+} candidates. The mean values are $\langle z \rangle = 0.51 \pm 0.03 \pm 0.04$ and $0.36 \pm 0.02 \pm 0.03$, respectively. Here, the last (systematic) errors reflect the uncertainty of R , and therefore are correlated. Then, taking into account the fitted background under the D^0 peak (4.6 ± 1.3 combinations), we obtain the mean z for ‘pure’ D^{*+} production as $\langle z \rangle = 0.55 \pm 0.04(stat) \pm 0.04(syst)$. This value may be compared with $\langle z \rangle = 0.59 \pm 0.03 \pm 0.08$ as observed at lower neutrino energies [4] or with $\langle z \rangle = 0.61 \pm 0.04$ for D mesons [5], and with about 0.5 for fragmentation of a 45 GeV charmed quark into a D^{*+} meson [6].

In a similar manner, for the Bjorken scaling variables we obtain $\langle x \rangle = 0.26 \pm 0.05(stat) \pm .01(syst)$ and $\langle y \rangle = 0.52 \pm 0.07(stat) \pm 0.01(syst)$, in agreement with the expected flat y distribution.

The D^{*+} could be products of D^{**0} decays (see reference [7] and references therein). A recent search for the production of such D^{**0} mesons in neutrino and antineutrino interactions at lower energies [4] only had one candidate D^{**0} from a signal of some 46 D^{*+} , and provided upper limits on the D^{**0} production rate. In our experimental conditions, we find that a search for D^{**0} production is complicated by a poorer mass resolution which is larger than the natural widths of the D^{**0} states, and by limited statistics. As a result, the production limits [4] are not improved by the present experiment.

4 D^{*+} Production Cross Section

Some of our candidate combinations in the V^0 sample have no K_S^0 in the D^0 decay but have an accompanying K_S^0 (see shaded entries in Figs. 2 and 3). We do not have any estimate of how often a D^{*+} will be accompanied by a K_S^0 . Therefore we omit these combinations when we estimate the D^{*+} production rate. Upon dropping these combinations and subtracting the single double peak entry from the fitted value, the observed effect reduces to 14.8 ± 4.6 events above the background (this estimate is conservative insofar as several double entries have been retained in the background).

The effect is significantly reduced by the loss of charged particles which interact in the bubble chamber before having a long enough track (L_{min}) for an accurate momentum measurement, $\sigma_p/p < 0.2$. In the E546 experiment performed in very similar experimental conditions [8], the minimum length was parametrized as $L_{min}(cm) = 9.7p^{0.5}$ (p in GeV) for charged particles with $\sigma_p/p < 0.3$. We have checked that this form provides an acceptable description of our high-energy data. Adding a factor of $\sqrt{3/2}$ for the tighter selection $\sigma_p/p < 0.2$, we determine momentum-dependent charged particle weights for the two runs (see the Introduction) by analyzing the ratio $N(L > L_{min})/N(L > 2L_{min})$, where N is the inclusive number of well measured charged particles with measured track length L , in different momentum intervals. For the three-prong and five-prong D^{*+} decay topologies (also counting the slow π^+), the mean weights correcting for charged decay products with $L < L_{min}$ are computed as 1.52 ± 0.07 and 2.44 ± 0.30 using the observed D^{*+} candidates in the peak.

The D^{*+} production is estimated to occur in $(5.6 \pm 1.8)\%$ of all neutrino charged current interactions. (In this calculation, the measured D^0 and D^{*+} branching fractions [2] are used, and the gamma and K_S^0 [1] detection efficiencies are taken into account.) At lower neutrino energies (about 50 GeV on average), the D^{*+} production rate has been measured as $(1.22 \pm 0.25)\%$ of neutrino charged current interactions [4]. Albeit with a considerable error, the threefold increase in incident neutrino energy above previously published results appears to result in a fivefold gain in D^{*+} yield per neutrino interaction.

To probe the energy dependence of D^{*+} production within the E632 data, we then select the events with estimated neutrino energy E_ν above 100 GeV, keeping some 55% of the charged-current sample with mean energy near 203 GeV. The corresponding mass and detachment plots, as illustrated in Figs 2d and 3d, show that the bulk of D^{*+} production occurs at highest neutrino energies. We estimate that D^{*+} mesons are produced in $(10.3 \pm 3.1)\%$ of all neutrino charged current interactions with $E_\nu > 100$ GeV, and in $(0.2 \pm 1.7)\%$

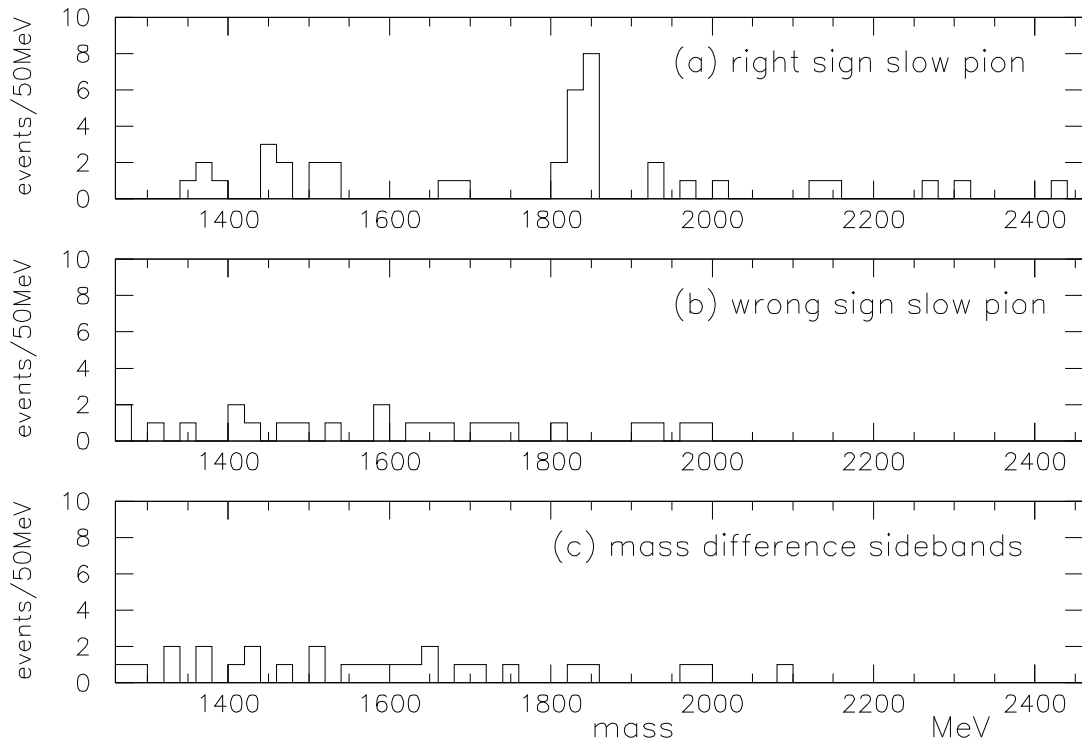


Figure 4: Combined $m(X^0)$ plots for the BEBC hydrogen and deuterium data with $E_\nu > 100$ GeV: (a) X^0 combinations tagged by a right–sign slow pion passing the D^*-D mass difference selection; (b) X^0 combinations tagged by a wrong–sign slow pion passing the mass difference selection; (c) X^0 combinations tagged by a right–sign pion with mass difference in the sidebands.

of interactions with $E_\nu < 100$ GeV which have a mean energy of 65 GeV.

An alternative probe of energy dependence of the D^{*+} cross section is to select the highest-energy neutrino interactions in BEBC (their number is considerable because of large overall statistics). For this, we select charged current interactions in hydrogen [9] and deuterium [10] with incident neutrino energy over 100 GeV and with event potential length in BEBC over 100 cm (1754 and 3372 events, respectively). We correct the event energy for missing neutrals by statistically balancing the event transverse momentum [11]. The mean neutrino energy for this selected subsample (146 GeV) is close to that for the full E632 sample. Applying the selections of Section 2, we obtain the mass distributions of Fig 4 showing a signal for D^{*+} production. For this high-energy BEBC subsample, we estimate that D^{*+} production occurs in $(3.8 \pm 1.1)\%$ of all neutrino charged current interactions.

It is interesting to examine the implications of the observed D^{*+} cross section for opposite–sign dileptons produced by high energy neutrinos. We adopt the world-average value of $(17.2 \pm 1.9)\%$ [2] for the D^+ semileptonic branching fraction, and then derive that

of the D^0 as $(6.8 \pm 0.8)\%$ using a recent measurement of the lifetime ratio: $\tau(D^+)/\tau(D^0) = 2.54 \pm 0.04$ [12]. Folding in the D^{*+} and D^{*0} branching fractions [2], we obtain $B(D^{*+} \rightarrow l^+ X) = (10.1 \pm 0.8)\%$, $B(D^{*0} \rightarrow l^+ X) = (6.8 \pm 0.8)\%$. Then, assuming that the D^{*+} and D^{*0} cross sections are equal, the $\mu^- \mu^+$ and $\mu^- e^+$ dileptons from D^* decays are predicted to occur in $(0.94 \pm 0.31)\%$ of all neutrino charged current interactions, and in $(1.74 \pm 0.54)\%$ of those with $E_\nu > 100$ GeV. These numbers are in excess of, though compatible with, the total dilepton yields as obtained in [8,13,14].

5 Conclusions

Charmed vector $D^{*+}(2010)$ meson decays are selected in a high-energy neutrino experiment with mean event energy of 141 GeV. Their production rate is measured as $(5.6 \pm 1.8)\%$ per neutrino charged current interaction, significantly exceeding that for lower neutrino energies. The mean fractional hadronic energy of the D^{*+} is 0.55 ± 0.06 , in good agreement with both the low-energy neutrino data and with the e^+e^- data for comparable energy of a fragmenting charmed quark.

Acknowledgements. We would like to thank Fermilab for providing the neutrino beam and for successful data taking periods. We also thank the E632 collaboration scanning and measuring teams for their invaluable contributions. We are grateful to the WA21 and WA25 Collaborations for allowing us to use their data. We thank the US Department of Energy and National Science Foundation and other funding agencies for their support. This investigation was supported in part by the International Science Foundation and the Russian Ministry of Science (grant J1Z100).

References

- [1] D. DeProspero et al. (E632), Phys. Rev. D50, 6691 (1994)
- [2] Particle Data Group, Phys. Rev. D54, no. 1 (1996)
- [3] J. Adler et al. (Mark III), Phys. Rev. Lett. 64, 2615 (1990)
- [4] A.E. Asratyan et al. (Big Bubble Chamber Neutrino Coll.), Z. Phys. C68, 43 (1995)
- [5] N. Ushida et al (E531), Phys. Lett. 121B, 292 (1983)
- [6] D. Buskulic et al. (ALEPH), Z. Phys. C62, 1 (1994); P. Aubreu et al. (DELPHI), Z. Phys. C59, 533 (1993); R. Akers et al. (OPAL), Z. Phys. C67, 27 (1995)
- [7] G. Crawford et al. (CLEO), Phys. Lett. 331B, 236 (1994)
- [8] H.C. Ballagh et al. (E546), Phys. Rev. D24, 7 (1981)
- [9] G.T. Jones et al. (WA21), Z. Phys. C51, 11 (1991)
- [10] D. Allasia et al. (WA25), Z. Phys. C37, 527 (1988)

- [11] M. Aderholz et al., Phys. Lett. 173B, 211 (1986)
- [12] P.L. Frabetti et al. (E687), Phys. Lett. 323B, 459 (1994)
- [13] V. Jain et al. (E632), Phys. Rev. D41, 2057 (1990)
- [14] A. Rabinovitz et al. (CCFR), Phys. Rev. Lett. 70, 134 (1993)